Reactivity of aluminum cluster anions with ammonia: Selective etching of Al_{11}^- and Al_{12}^-

Andrej Grubisic,[1] Xiang Li,[1] Gerd Gantefoer,[1,a)] Kit H. Bowen,[1,b),c)] Hansgeorg Schnöckel,[2,b)] Francisco J. Tenorio,[3,b)] and Ana Martinez[4,b)]
[1]*Department of Chemistry, Johns Hopkins University, Baltimore, Maryland 21218, USA*
[2]*Institut für Anorganische Chemie, Karlsruhe Universität, Karlsruhe 76128, Germany*
[3]*Departamento de Ciencias Exactas y Tecnología, Centro Universitario de Los Lagos, Universidad de Guadalajara, Jalisco 47460, Mexico*
[4]*Departamento de Materia Condensada y Criogenia, Instituto de Investigaciones en Materiales, Universidad Nacional Autónoma de México, Coyoacán 04510, Distrito Federal, Mexico*

(Received 3 August 2009; accepted 7 October 2009; published online 11 November 2009)

Reactivity of aluminum cluster anions toward ammonia was studied via mass spectrometry. Highly selective etching of Al_{11}^- and Al_{12}^- was observed at low concentrations of ammonia. However, at sufficiently high concentrations of ammonia, all other sizes of aluminum cluster anions, except for Al_{13}^-, were also observed to deplete. The disappearance of Al_{11}^- and Al_{12}^- was accompanied by concurrent production of $Al_{11}NH_3^-$ and $Al_{12}NH_3^-$ species, respectively. Theoretical simulations of the photoelectron spectrum of $Al_{11}NH_3^-$ showed conclusively that its ammonia moiety is chemisorbed without dissociation, although in the case of $Al_{12}NH_3^-$, dissociation of the ammonia moiety could not be excluded. Moreover, since differences in calculated $Al_n^- + NH_3$ (n=9–12) reaction energies were not able to explain the observed selective etching of Al_{11}^- and Al_{12}^-, we concluded that thermodynamics plays only a minor role in determining the observed reactivity pattern, and that kinetics is the more influential factor. In particular, the conversion from the physisorbed $Al_n^-(NH_3)$ to chemisorbed $Al_nNH_3^-$ species is proposed as the likely rate-limiting step. © *2009 American Institute of Physics*. [doi:10.1063/1.3256236]

I. INTRODUCTION

Aluminum clusters have attracted considerable interest over the past couple of decades. These studies were aimed at understanding the behavior of aluminum clusters in the size-range that lies between individual atoms and the bulk.[1–9] It was realized early on that bonding within aluminum clusters can be explained reasonably well in terms of the jelliumlike shell model.[10] According to this model, the atoms donate their valence electrons to a pool of delocalized electrons that are free to move in the electrostatic potential well generated by the resulting positively charged cores. This nearly free electron cloud masks the charge of neighboring cations; thus gluing the cluster together. The situation resembles that found in bulk metals, where the metallic bond is thought to dominate. Unlike in a bulk metal, however, in clusters, quantum confinement effects lead to formation of electronic shells similar to those encountered in atoms. Clusters with completely filled shells have been found to be more stable than those with incomplete shells. The number of electrons required to fill consecutive shells are 2, 8, 18, 20, 34, 40, 70, etc. Since aluminum is trivalent, compositions such as Al_7^+, Al_{13}^-, and Al_{23}^- are expected to be relatively stable, i.e., "magic."[1,11]

A number of experimental studies have observed such shell closures in the case of aluminum clusters.[4–8,12–14] Some sizes with closed shells have been shown to possess remarkable stability. In particular, Al_{13}^-, with its closed shell of 40 valence electrons, has been shown to resist attack even by such reactive species as O_2.[7,14,15] Its apparent stability led to the idea of exploiting these clusters as building blocks of cluster-assembled materials.[16–18] This prospect resulted in renewed interest in aluminum cluster ions and their reactivity.[15,19–24]

In the present paper, we explore the reactivity of aluminum cluster anions with ammonia. Most strikingly, highly selective etching of Al_{11}^- and Al_{12}^- was found at low concentrations of ammonia, while at sufficiently high concentrations of ammonia, all other sizes of aluminum cluster anions, except for Al_{13}^-, were also seen to deplete. The disappearance of Al_{11}^- and Al_{12}^- was accompanied by the concurrent production of $Al_{11}NH_3^-$ and $Al_{12}NH_3^-$ species, respectively. In an earlier study of the reactivity of neutral aluminum clusters with ammonia, Kaya and co-workers[3] observed enhanced rates of physisorbed adduct formation for $Al_{n<13}$ clusters compared with those for $Al_{n\geq13}$. However, no particularly drastic increase was noted for sizes, n=11 and 12. In a study of the reactivity of anionic aluminum clusters with propene, Castleman and co-workers[19] observed markedly enhanced reactivity for Al_{12}^- (as well as for Al_{15}^-, Al_{18}^-, and Al_{21}^-), but not for Al_{11}^-. They attributed the reactivity of the series mainly to geometric factors, i.e., active sites on the surface of these clusters, as well as to electronic factors in the case of Al_{12}^-. Similar conclusions were also reached in

a)Present address: Department of Physics, Konstanz University, Konstanz, Germany.
b)Authors to whom correspondence should be addressed.
c)Electronic mail: kbowen@jhu.edu.

 © 2009 American Institute of Physics

their subsequent work on reactions of Al_n^- clusters with H_2O.[25] While the relative inertness of Al_{13}^- to reaction can no doubt be understood in terms of its electronic shell closure, the specific reactivities of other aluminum cluster anion sizes with these molecules are not well explained by the shell model. Thus, deeper insight into the physical and chemical interactions between aluminum cluster anions and small molecules is necessary in order to elucidate the observed size-specific reactivity of aluminum cluster anions. Here, we employ a synergistic combination of theory and experiment to explore the basis of the enhanced reactivity of Al_{11}^- and Al_{12}^- with ammonia.

II. METHODS

A. Experimental

Reactivity studies were performed by exposing aluminum cluster anions to ammonia gas and monitoring the resultant products with a linear time-of-flight mass spectrometer (TOF-MS). Aluminum cluster anions were generated using a pulsed arc cluster ionization source, details of which are given elsewhere.[26] Briefly, the source consists of a grounded aluminum cathode and a copper anode. A 30–40 μs long 100 V pulse applied to the anode creates a discharge in the narrow gap between the two electrodes, and this vaporizes aluminum off the cathode. A well synchronized burst of helium gas (5–10 atm) entrains the resulting plasma and directs it down a 10–15 cm condensation channel, where the mixture cools and forms aluminum clusters and aluminum cluster ions. A plume of neat ammonia gas (1–3 atm) dosed from a second pulsed valve then intercepts the clusters at about a third of their way through the channel. This ensures that the clusters have had sufficient time to form prior to ammonia exposure and will at the same time remain within the spatial confines of the channel sufficiently long to react with ammonia molecules. The reaction products as well as any remaining reactant species are next carried into the differentially pumped Wiley–McLaren region of the TOF-MS, where the anionic components of the mixture are extracted and mass analyzed. Mass resolution typically attained by our MS is ~400 amu.

The cluster anions of interest can also be studied in an anion photoelectron spectrometer located at the end of the mass separating stage of our apparatus. In anion photoelectron spectroscopy a beam of mass-selected negative ions is intercepted by a fixed-frequency photon beam and the kinetic energy of the resultant photodetached electrons is analyzed. The photodetachment process is governed by the energy-conserving relationship $h\nu$=EBE+EKE, where $h\nu$ is the photon energy, EBE is the electron binding energy, and EKE is the electron kinetic energy. In this way electronic structure information can be obtained. For the present study the fourth (266 nm, 4.661 eV) harmonic of an Nd:YAG (yttrium aluminum garnet) laser was employed for photodetachment. The resulting electrons were energy-analyzed by a magnetic-bottle type photoelectron spectrometer with a typical resolution of ~35 meV at 1 eV EKE. The details of our apparatus are described elsewhere.[27]

B. Theoretical

Density functional theory (DFT) as implemented in GAUSSIAN 03 (Ref. 28) was used for all the calculations. The hybrid, three parameter B3LYP (Refs. 29–31) functional was used for the calculation of complete optimizations, without symmetry constraints. Los Alamos LANL2DZ effective core pseudopotentials with a split valence double-ζ basis set were employed.[32–39] Harmonic frequency analyses permitted us to verify optimized minima.

Owing to the fact that an adequate number of isomers were explored during the initial stages of the study, we were able to extensively explore the potential energy surface in our search for the global minimum. The number of initial geometries examined here is great enough to reliably identify the global minima. Several initial geometries were optimized, including all possible bonds between aluminum clusters and NH_3. We also optimized several dissociated adducts (with NH_3 dissociated in several ways). The structures reported here are those with the lowest energy values. In order to compute the vertical electron detachment energies (VDEs) of anionic species, further single-point calculations were required. The P3 electron propagator approximation was employed.[40,41] The most stable structures from density functional calculations were reexamined with additional geometry optimizations; first with the same LANL2DZ basis set and later with the 6-31G and 6-311G(d,p) basis set[35] at the MP2 (Ref. 42) level. No substantial structural differences between the results were found. Density functional and MP2 geometries were employed in correlated, *ab initio*, electron propagator calculations of the VDE values for the $Al_{11}NH_3^-$ systems. For each value of VDE, which was calculated with the electron propagator, there corresponds a Dyson orbital

$$\Phi_{\mathrm{Dyson}}(x_1) = N \cdot \frac{1}{2} \cdot \int \Psi_{\mathrm{anion}}(x_1, x_2, x_3, \ldots, x_N) \cdot \Psi^*_{\mathrm{neutral}}(x_2, x_3, x_4, \ldots, x_N) dx_2 dx_3 dx_4 \ldots dx_N,$$

where N is the number of electrons in the anion and x_i is the space-spin coordinate of electron i. The Dyson orbital thus represents the change in electronic structure associated with vertical electron detachment. The normalization integral of the Dyson orbital is known as the pole strength and is given by

$$p = \int |\Phi_{\mathrm{Dyson}}(x)|^2 dx.$$

In the zeroth order electron propagator, values for VDE are given by Koopmans's theorem (that is, VDE values equal negatives of occupied, canonical, Hartree–Fock orbital energies of the anion); Dyson orbitals equal canonical, Hartree–Fock orbitals, and pole strengths equal unity. In the present, correlated calculations, however, Dyson orbitals are, in general, linear combinations of Hartree–Fock orbitals and pole strengths lie between 0 and 1. When pole strengths lie between 0.85 and unity, these approximations are validated.

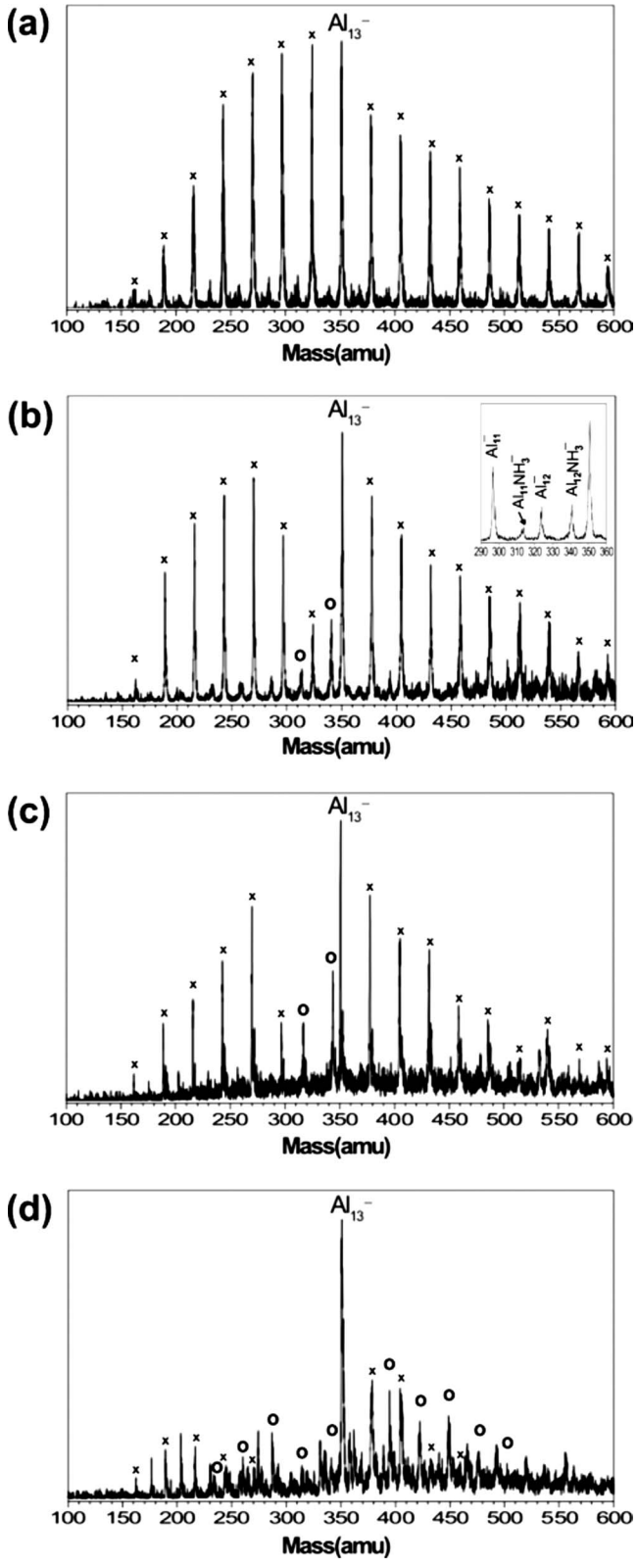

FIG. 1. Typical mass spectra of anionic products of Al_n^-+NH_3 reactions. The effect of the increasing NH_3 concentration is shown in series from (a) through (d). "x" and "o" denote Al_n^- and $Al_nNH_3^-$ species, respectively.

III. RESULTS AND DISCUSSION

A typical mass spectrum of aluminum cluster anions generated during this work is shown in Fig. 1(a). Upon exposure of aluminum cluster anions to a small amount of ammonia gas (low backing pressure) the intensity of Al_{12}^- is observed to diminish and is accompanied by the appearance of a peak at a 17 amu higher mass [Fig. 1(b) and inset]. Analogous, but slightly less pronounced behavior is observed for Al_{11}^- as well. Since ammonia has a mass of 17 amu, we infer that the stoichiometries of the two nascent species correspond to $Al_{12}NH_3^-$ and $Al_{11}NH_3^-$, respectively. Upon increasing the pressure of ammonia gas, the intensities of both Al_{11}^- and Al_{12}^- decrease further to a point where Al_{12}^- almost entirely disappears [Fig. 1(c)]. A concomitant increase in NH_3-containing species is observed. However, their intensities never reach the original intensity levels of Al_{11}^- and Al_{12}^- reactants, suggesting that NH_3 attachment is accompanied by sizable electron detachment (anion loss) channels as well. Upon further increasing the ammonia concentration [Fig. 1(d)], both Al_{11}^- and Al_{12}^- completely disappear, and the intensities of all other Al_n^- ions decrease precipitously. Considering the trends among ion intensities as the ammonia concentration increases [Figs. 1(a)–1(d)], $Al_{n<13}^-$ sizes are seen to diminish more at a lower ammonia concentration than those of $Al_{n>13}^-$, while at all ammonia concentrations, Al_{13}^- remains relatively unreactive. The following series lists Al_n^- ($n<20$) clusters in a decreasing order of reactivity toward NH_3: $Al_{12}^- > Al_{11}^- \gg Al_{n<11}^- > Al_{n>13}^- \gg Al_{13}^-$. Among the negatively charged reaction products, $Al_n(NH_3)^-$ species are observed to accompany reductions in Al_n^- intensities. Reaction side products that are observed in the mass spectra include Al_nH^- species as well as Al_nN^- species, the latter occurring especially at higher ammonia concentrations and among smaller Al_n^- clusters.

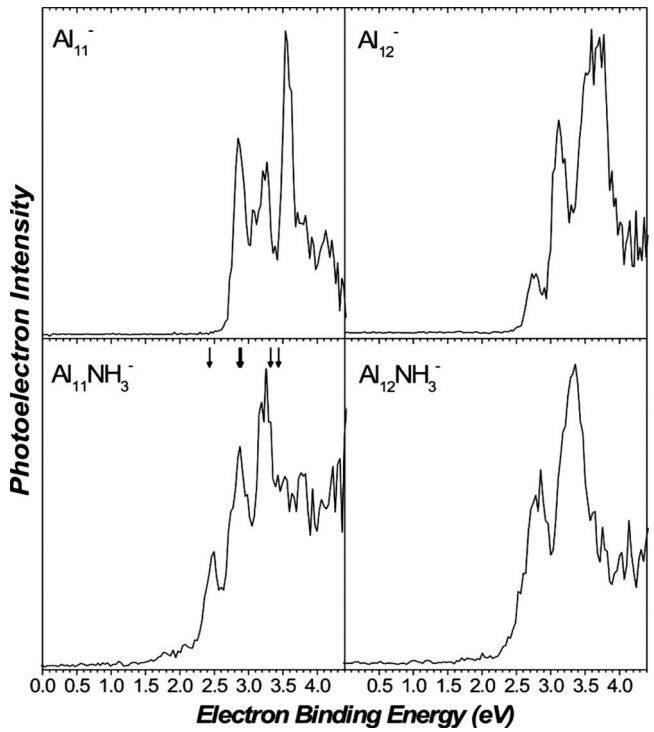

FIG. 2. Photoelectron spectra of $Al_{11}NH_3^-$ and $Al_{12}NH_3^-$ (bottom row) together with Al_{11}^- and Al_{12}^- (top row) recorded with 266 nm photons. Arrows in the spectrum of $Al_{11}NH_3^-$ mark calculated transitions (See Table I).

Photoelectron spectra of $Al_{11}NH_3^-$ and $Al_{12}NH_3^-$ are shown in Fig. 2. Their comparison with the photoelectron

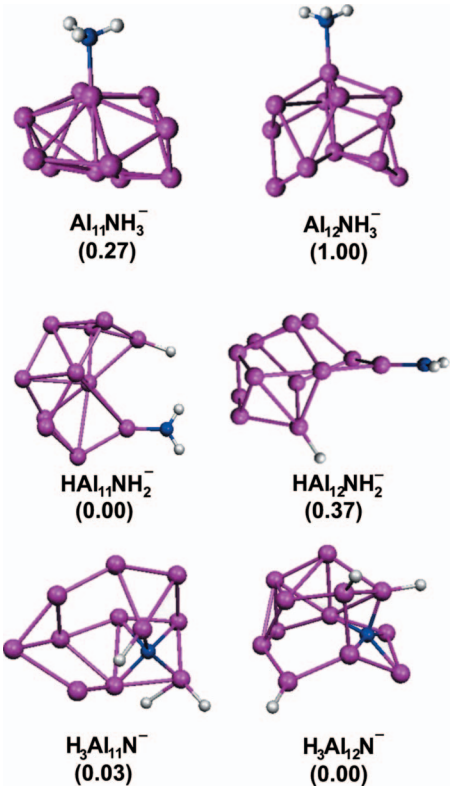

FIG. 3. Minimum energy structures of three distinct chemisorbed isomer classes. The top row shows $Al_nNH_3^-$ adducts, while the middle and bottom rows show species with a partially and fully dissociated ammonia molecule, $HAl_nNH_2^-$ and $H_3Al_nN^-$, respectively (n=11–12). Relative energy values for a given size are given in parentheses. All units are in eV.

spectra of the bare aluminum clusters, Al_{11}^- and Al_{12}^-, (also in Fig. 2) likely precludes NH_3 acting merely as a "solvent" in an anion-solvent complex. In such a complex, the largely unchanged spectral profile of the anionic chromophore would shift to a higher EBE value due to solvent stabilization of the excess charge on the chromophore. In the photoelectron spectra of neither Al_{11}^- versus $Al_{11}NH_3^-$, nor Al_{12}^- versus $Al_{12}NH_3^-$ are their spectral profiles unchanged, nor are the spectra of $Al_{11}NH_3^-$ and $Al_{12}NH_3^-$ shifted to higher EBE values relative to those of their chromophores, Al_{11}^- or Al_{12}^-, respectively. Furthermore, the onsets of photoelectron intensities are, for both sizes, lower in the cases of ammoniated species ($Al_{11}NH_3^-$: 2.2 ± 0.1 eV; $Al_{12}NH_3^-$: 2.4 ± 0.1 eV) than in the cases of bare aluminum species (Al_{11}^-: 2.70 ± 0.05 eV; Al_{12}^-: 2.55 ± 0.05 eV). The observation implies a destabilizing effect of the bound NH_3 molecule on the excess negative charge in the cluster, perhaps due to the preferential formation of a Al–N bond. Such a bond would force the more electronegative element closer to the negative charge, thereby explaining the observed reduction in electron's binding energy. The photoelectron spectra of fully deuterated species ($Al_{11}ND_3^-$ and $Al_{12}ND_3^-$) were also recorded (not shown) and are identical to those of their respective nondeuterated species, thus suggesting that the resolved transitions are mainly due to electronic rather than vibrational transitions.

Calculated minimum energy geometries for three classes of $Al_nNH_3^-$ (n=11–12) isomers are shown in Fig. 3. The top row shows the structures of the adducts $Al_nNH_3^-$. The middle row shows structures containing partially dissociated ammonia molecule $HAl_nNH_2^-$, while the bottom row shows structures with fully dissociated ammonia molecule $H_3Al_nN^-$. Their relative total energies are shown in parentheses in each case. Our calculations indicate that isomer stability tends to increase with the degree of dissociation, that at least one Al–N bond is formed in all structures, and that the number of such bonds increases with the extent of NH_3 dissociation.

Photoelectron spectral transitions for three minimum energy isomeric structures of the $[Al_{11}–NH_3]^-$ system were calculated and are given in Table I. Predictions based on electron propagator theory offered a reliable means of identifying its structure. An excellent match was found between the experimentally observed transitions and those theoretically predicted for the chemisorbed $Al_{11}NH_3^-$ adduct structure (see arrows in Fig. 2). Thus, a single structure appears to

TABLE I. Calculated photoelectron spectral transitions (eV) for several minimum energy structures. In the cases of the $[Al_{12}–NH_3]^-$ systems, the tabulated transition energies are given as VDE values.

$[Al_{11}–NH_3]^-$ systems[a]				$[Al_{12}–NH_3]^-$ systems[b]			
$Al_{11}NH_3^-$	$HAl_{11}NH_2^-$	$H_3Al_{11}N^-$	Expt.[c]	$Al_{12}NH_3^-$	$HAl_{12}NH_2^-$	$H_3Al_{12}N^-$	Expt.[c]
2.47	2.61	2.54	2.5	2.22	2.67	2.92	2.8
(0.90)	(0.89)	(0.87)					
2.87	3.16	2.56	2.9				
(0.88)	(0.88)	(0.87)					
2.88	3.20	2.98	3.2				
(0.89)	(0.89)	(0.87)					
3.31	3.24	3.23					
(0.88)	(0.89)	(0.87)					
3.42	3.24	3.50					
(0.89)	(0.89)	(0.85)					
3.55	3.64	3.72					
(0.90)	(0.90)	(0.85)					

[a]Electron propagator theory (P3 results, LANL2DZ basis set). Pole strengths are included in parentheses.
[b]DFT.
[c]Uncertainty of ±0.1 eV.

TABLE II. Calculated reaction energies for several $Al_x^- + NH_3$ reaction channels (in eV).

Reaction	Reacting Al_x^- cluster species			
	Al_9^-	Al_{10}^-	Al_{11}^-	Al_{12}^-
$Al_x^- + NH_3 \rightarrow Al_xNH_3^-$	−0.44	−0.55	−0.67	−0.43
$Al_x^- + NH_3 \rightarrow HAl_xNH_2^-$	−1.58	−0.98	−0.94	−1.06
$Al_x^- + NH_3 \rightarrow Al_xH^- + NH_2$	+1.93	+2.38	+2.55	+2.02
$Al_x^- + NH_3 \rightarrow Al_xN^- + 3/2H_2$	−0.83	−0.75	+0.07	−0.35

explain the photoelectron spectrum of $Al_{11}NH_3^-$. We conclude that the observed reaction product of $Al_{11}^- + NH_3$ reaction is the adduct, $Al_{11}NH_3^-$, in which its ammonia moiety is chemisorbed without dissociation. Since the total energy of $Al_{11}NH_3^-$ was calculated to be higher than that of $HAl_{11}NH_2^-$ (see values in Fig. 3), we suspect that there is a barrier between the two which prevents $Al_{11}NH_3^-$ from going to $HAl_{11}NH_2^-$ (our calculation finds it to be 1.08 eV high). Turning to $Al_{12}NH_3^-$, a similarly reliable simulation of its photoelectron spectrum was not possible with electron propagator theory, since it is limited to singlet species. Instead, DFT was employed to obtain the first photoelectron spectral transition (VDE) for three isomers. The experimental VDE value of 2.8 ± 0.1 eV agrees best with predictions for the partially and fully dissociated ammonia species, $HAl_{12}NH_2^-$ and $H_3Al_{12}N^-$ (see values in Table I). However, identification based on a single transition, together with DFT's lower accuracy, precludes a definitive dismissal of the chemisorbed ammonia adduct, $Al_{12}NH_3^-$ from the pool of possible structures.

To investigate the role of thermodynamics in the observed enhanced reactivity of Al_{11}^- and Al_{12}^- toward NH_3, several possible $Al_{n=9-12}^- + NH_3$ reaction channels were considered. Their calculated reaction energies are summarized in Table II. The chemisorption of NH_3 on Al_n^- clusters is thermodynamically favorable ($\Delta E \sim -0.5$ eV) for all theoretically studied sizes (n=9–12). So also is the consequent dissociation of the ammonia molecule on the cluster's surface. Most importantly however, no significant differences were found between reaction energies involving Al_{11}^- and Al_{12}^- on one hand, and Al_9^- and Al_{10}^- on the other. Thus, thermodynamics likely plays only a minor role in the observed enhanced reactivity of Al_{11}^- and Al_{12}^- toward NH_3. Furthermore, the formation of Al_nH^- via the $Al_n^- + NH_3$ reaction is thermodynamically unfavorable ($\Delta E > 1.9$ eV), and this is likely not a major pathway by which the observed Al_nH^- clusters form. They are more likely formed due to the presence of excess ammonia molecules in the discharge region from the previous gas injection event. Ammonia discharges are a well known source of H^- anions. Al_nN^- formation, on the other hand, is at least slightly thermodynamically favorable, except for Al_{11}^- for which nitride formation appears slightly endothermic.

Since thermodynamic arguments cannot explain the observed size-specific reactivity of aluminum cluster anions toward ammonia, we infer that the underlying reasons are likely kinetic in nature. Kinetics has been invoked as the root cause of the observed size-specific reactive behavior of clusters in many previous studies.[43] Calculations indicate that chemisorbed products (both intact and dissociated) are thermodynamically favored for all studied sizes in reactions between Al_n^- and NH_3; yet only adducts in case of Al_{11}^- and Al_{12}^- are experimentally observed. The empirical evidence therefore suggests that one of the elementary steps leading to the formation of chemisorbed adduct species is likely the rate-limiting one.

Initially, when a polar ammonia molecule approaches the negatively charged cluster, electrostatic attraction between the two moieties leads to the creation of a physisorbed species [Eq. (1)]. Due to the long range nature of the electrostatic forces it is unlikely that properties other than the overall charge on the cluster would significantly influence the interaction of clusters with the ammonia molecule. Hence, pronounced size-specific behavior would not be expected to accompany the formation of the physisorbed product. In a second step, the physisorbed precursor converts into a chemisorbed product [Eq. (2)]. A relatively strong Al–N bond is formed in this step ($\Delta E \sim -0.5$ eV). Since its formation requires that the ammonia molecule comes close to a suitable aluminum atom (or atoms), size-specific behavior due to either surface active sites, cluster's electronic structure or both, can be envisioned as being important in this step. We thus propose the following reaction mechanism for the formation of aluminum cluster anions with a chemisorbed NH_3 molecule:

$$Al_n^- + NH_3 \rightarrow Al_n^-(H_3N) \quad \text{fast}, \tag{1}$$

$$Al_n^-(H_3N) \rightarrow Al_nNH_3^- \quad \text{slow}. \tag{2}$$

The existence of a barrier in Eq. (2) can be rationalized by noting that in the physisorbed species the dipole moment of ammonia likely orients the molecule in a way where the nitrogen atom points away from the aluminum cluster anion. To form the Al–N bond present in the chemisorbed adduct, the ammonia molecule has to reorient itself (by rotating or undergoing an umbrella-flip) into an energetically less favorable orientation, where the more electronegative element (i.e., nitrogen) faces the negative charge. The experimentally observed trend in reactivity of Al_n^- clusters toward ammonia therefore suggests that the barriers for the initial formation of the chemisorbed adduct [Eq. (2)] increase in the following order: $Al_{12}^- < Al_{11}^- \ll Al_{n<11}^- < Al_{n>13}^- \ll Al_{13}^-$. Since Al_{13}^- remains relatively unscathed even in harshest conditions (i.e., highest concentration of NH_3) a substantial barrier is inferred for the reaction of Al_{13}^- with NH_3. The cluster's inertness can be attributed to a combination of electronic (closed shell) and geometric stability (no active sites). The reasons for low barriers in case of Al_{11}^- and Al_{12}^- are less obvious.

In the case of Al_{12}^-, however, 37 valence electrons and its consequent striving to achieve an electronic shell closure may explain its tendency to react with electron-rich (nucleophilic) molecules. Similar behavior was previously observed in Al_n^+ clusters interacting with a different lone pair-containing molecule, i.e., water.[24] In that study a magic mass spectral peak was observed for the $Al_{13}(H_2O)^+$ complex, even though no such magic peak was observed for Al_{13}^+ with

its 38 valence electrons. The enhanced intensity of the complex was attributed to formation of a coordinate bond, in which the water molecule shares the equivalent of one of its lone electron pairs with the electron-deficient Al_{13}^+, thereby effectively making it a 40 electron system. In case of Al_{12}^- three electrons would be needed for achieving a closed shell, whereas a single lone pair on the ammonia can only provide two. Nevertheless, previous studies have shown that the stability can be gained merely by approaching the closed shell, even though it is not actually attained.[44] Thus, electronic reasons may contribute to the lower barrier observed for chemisorption of electron donating molecules onto the Al_{12}^- cluster. The two recent studies on reactivity of aluminum cluster anions toward propene and water corroborate this suggestion.[19,25] There, a similarly enhanced reactivity of Al_{12}^- was attributed to a low-lying lowest unoccupied molecular orbital, which facilitates a reaction with electron-rich molecules. In addition, geometric factors were proposed to complement electronic ones. Specifically, the apical aluminum atom in Al_{12}^- was identified as the active site on the surface of the cluster, where the initial adduct formation takes place. Thus, there is evidence from three experiments which find Al_{12}^- to be inherently reactive at least toward electron-donating/electron-rich molecules. On the other hand, the slightly lower, yet still substantial reactivity of Al_{11}^- appears limited to NH_3. Note that the cluster appears unreactive even toward the most related nucleophile, e.g., water.[25] This implies that its reactivity stems from an electronic or geometric match between the two reactants rather than some inherent instability of Al_{11}^-.

IV. CONCLUSION

Selective etching of Al_{11}^- and Al_{12}^- was observed upon exposure of aluminum cluster anions to moderate ammonia concentrations. $Al_{11}NH_3^-$ and $Al_{12}NH_3^-$ species each with a chemisorbed ammonia molecule were identified as the main reaction products. A two-step reaction mechanism was proposed, wherein an NH_3 molecule initially physisorbs onto the cluster and subsequently chemisorbs by forming a relatively strong Al–N bond. The conversion from the physisorbed precursor into the chemisorbed adduct is proposed as the rate-determining step. The putative barrier may stem from the need to flip the NH_3 molecule from its energetically more favorable orientation with H atoms facing the negatively charged cluster in the physisorbed species into one, where the N atom faces the cluster in the chemisorbed adduct. The following order of barrier heights was inferred from the observed reactivity patterns: $Al_{12}^- < Al_{11}^- \ll Al_{n<11}^- < Al_{n<13}^- \ll Al_{13}^-$. Thus, it appears that varying barrier heights govern the selective etching observed in this work. Lastly, it is interesting to speculate that such barriers are likely to be much smaller in the case of neutral clusters or even entirely absent in the case of positively charged clusters, where orientation of the ammonia molecule is likely to be the same in the physisorbed and chemisorbed states.

ACKNOWLEDGMENTS

K.B. gratefully acknowledges the Air Force Office of Scientific Research for its support of this work. G.G. and H.S. also acknowledge the Deutsche Forschungsgemeinschaft. The theoretical parts of this study were made possible due to the funding by DGAPA-PAPIIT (Grant No. IN124602-3), Consejo Nacional de Ciencia y Tecnología CONACyT (Grant No. 222506), and resources provided by the Instituto de Investigaciones en Materiales IIM. The calculations were carried out using a KanBalam supercomputer, provided by DGSCA, UNAM. In addition, the theoretical portions of the study were partially supported by PROMEP/103.5/08/2919.

[1] W. A. de Heer, Rev. Mod. Phys. **65**, 611 (1993).
[2] P. Jena, S. N. Khanna, and B. K. Rao, *Physics and Chemistry of Finite Systems: From Clusters to Crystals* (Kluwer, Dordrecht, 1992).
[3] K. Fuke, S. Nonose, N. Kikuchi, and K. Kaya, Chem. Phys. Lett. **147**, 479 (1988).
[4] D. M. Cox, D. J. Trevor, R. L. Whetten, and A. Kaldor, J. Phys. Chem. **92**, 421 (1988).
[5] M. F. Jarrold and J. E. Bower, J. Chem. Phys. **85**, 5373 (1986).
[6] M. F. Jarrold and J. E. Bower, J. Chem. Phys. **87**, 5728 (1987).
[7] R. E. Leuchtner, A. C. Harms, and A. W. Castleman, Jr., J. Chem. Phys. **94**, 1093 (1991).
[8] W. A. Saunders, P. Fayet, and L. Woste, Phys. Rev. A **39**, 4400 (1989).
[9] S. A. Ruatta, L. Hanley, and S. L. Anderson, Chem. Phys. Lett. **137**, 5 (1987).
[10] W. D. Knight, K. Clemenger, W. A. de Heer, W. A. Saunders, M. Y. Chou, and M. L. Cohen, Phys. Rev. Lett. **52**, 2141 (1984).
[11] M. Y. Chou and M. L. Cohen, Phys. Lett. A **113**, 420 (1986).
[12] J. Akola, M. Manninen, H. Häkkinen, U. Landman, X. Li, and L.-S. Wang, Phys. Rev. B **62**, 13216 (2000).
[13] E. Cottancin, M. Pellarin, J. Lerme, B. Baguenard, B. Palpant, J. L. Vialle, and M. Broyer, J. Chem. Phys. **107**, 757 (1997).
[14] R. L. Hettich, J. Am. Chem. Soc. **111**, 8582 (1989).
[15] R. Burgert, H. Schnöckel, A. Grubisic, X. Li, S. T. Stokes, K. H. Bowen, G. F. Ganteför, B. Kiran, and P. Jena, Science **319**, 438 (2008).
[16] S. N. Khanna and P. Jena, Phys. Rev. B **51**, 13705 (1995).
[17] K. Hoshino, K. Watanabe, Y. Konishi, T. Taguwa, A. Nakajima, and K. Kaya, Chem. Phys. Lett. **231**, 499 (1994).
[18] W.-J. Zheng, O. C. Thomas, T. P. Lippa, S.-J. Xu, and K. H. Bowen, Jr., J. Chem. Phys. **124**, 144304 (2006).
[19] D. E. Bergeron, A. W. Castleman, Jr., N. O. Jones, and S. N. Khanna, Chem. Phys. Lett. **415**, 230 (2005).
[20] D. E. Bergeron, A. W. Castleman, Jr., T. Morisato, and S. N. Khanna, Science **304**, 84 (2004).
[21] D. E. Bergeron, P. J. Roach, A. W. Castleman, Jr., N. O. Jones, and S. N. Khanna, Science **307**, 231 (2005).
[22] R. Burgert, H. Schnöckel, M. Olzmann, and K. H. Bowen, Jr., Angew. Chem., Int. Ed. **45**, 1476 (2006).
[23] R. Burgert, S. T. Stokes, K. H. Bowen, and H. Schnöckel, J. Am. Chem. Soc. **128**, 7904 (2006).
[24] T. P. Lippa, S. A. Lyapustina, S.-J. Xu, O. C. Thomas, and K. H. Bowen, Chem. Phys. Lett. **305**, 75 (1999).
[25] P. J. Roach, W. H. Woodward, A. W. Castleman, Jr., A. C. Reber, and S. N. Khanna, Science **323**, 492 (2009).
[26] H. R. Siekmann, C. Lueder, J. Faehrmann, H. O. Lutz, and K. H. Meiwes-Broer, Z. Phys. D: At., Mol. Clusters **20**, 417 (1991).
[27] M. Gerhards, O. C. Thomas, J. M. Nilles, W.-J. Zheng, and K. H. Bowen, J. Chem. Phys. **116**, 10247 (2002).
[28] M. J. Frisch, G. W. Trucks, H. B. Schlegel *et al.*, GAUSSIAN 03, Revision B.05 (Gaussian, Inc., Pittsburgh, PA, 2003).
[29] A. D. Becke, Phys. Rev. A **38**, 3098 (1988).
[30] B. Miehlich, A. Savin, H. Stoll, and H. Peuss, Chem. Phys. Lett. **157**, 200 (1989).
[31] C. Lee, W. Yang, and R. G. Parr, Phys. Rev. B **37**, 785 (1988).
[32] P. J. Hay and W. R. Wadt, J. Chem. Phys. **82**, 270 (1985).
[33] P. J. Hay and W. R. Wadt, J. Chem. Phys. **82**, 299 (1985).
[34] W. R. Wadt, J. Chem. Phys. **82**, 284 (1985).

[35] R. Krishnan, J. S. Binkley, R. Seeger, and J. A. Pople, J. Chem. Phys. **72**, 650 (1980).
[36] J.-P. Blaudeau, M. P. McGrath, L. A. Curtiss, and L. Radom, J. Chem. Phys. **107**, 5016 (1997).
[37] T. Clark, J. Chandrasekhar, G. W. Spitznagel, and P. R. Schleyer, J. Comput. Chem. **4**, 294 (1983).
[38] M. J. Frisch, J. A. Pople, and J. S. Binkley, J. Chem. Phys. **80**, 3265 (1984).
[39] A. D. McLean and G. S. Chandler, J. Chem. Phys. **72**, 5639 (1980).
[40] J. V. Ortiz, J. Chem. Phys. **104**, 7599 (1996).
[41] A. M. Ferreira, G. Seabra, O. Dolgounitcheva, V. G. Zakrewski, and J. V. Ortiz, *Quantum-Mechanical Prediction of Thermochemical Data* (Kluwer, Dordrecht, 2001).
[42] M. Head-Gordon, J. A. Pople, and M. J. Frisch, Chem. Phys. Lett. **153**, 503 (1988).
[43] M. B. Knickelbein, Annu. Rev. Phys. Chem. **50**, 79 (1999) (and references therein).
[44] O. C. Thomas, W.-J. Zheng, S.-J. Xu, and K. H. Bowen, Phys. Rev. Lett. **89**, 213403 (2002).

The Journal of Chemical Physics is copyrighted by the American Institute of Physics (AIP). Redistribution of journal material is subject to the AIP online journal license and/or AIP copyright. For more information, see http://ojps.aip.org/jcpo/jcpcr/jsp